Influence of light supplement on duck sternal calcification from integrated analysis of metabolome and transcriptome

Q. F. Wu,[*,†,1] H. H. Liu,[*,1] Q. L. Yang,[*] F. J. Pu,[*] B. Wei,[*] L. Y. Wang,[*] J. P. Li,[*] B. Hu,[*] J. W. Hu,[*] R. P. Zhang,[*] C. C. Han,[*] H. He,[*] B. Kang,[*] H. Y. Xu,[*] S. Q. Hu,[*] J. W. Wang,[*] and L. Liang [*,2]

[*]*Farm Animal Genetic Resources Exploration and Innovation Key Laboratory of Sichuan Province, College of Animal Science and Technology, Sichuan Agricultural University, Chengdu, 611130, China; and* [†]*Ministry of Agriculture, Forestry and Food Engineering, Yibin University, Yibin, 644000, China*

ABSTRACT Calcification of bones is the critical process of bone development in birds, which is very important for sustaining the normal biological function of bones. Light is one of the vital factors affecting bone development, but whether light intensity affects bone calcification and the underlying mechanism is still unknown. In this study, we used duck sternum as a model to analyze the calcification process under different light regimes. In addition, the underlying mechanism was also illustrated by integrating metabolomics and transcriptome methods.

The experiment lasted from 14 to 51 d of duck age. The control group (**LP1**) kept light intensity 2 lx during the whole experiment. The two light supplement groups (LP2, LP3) were given light with the intensity of 70 lx at different time (14−29 d for LP2, 14−43 d for LP3). Samples were collected at 52 d of duck age. Sternal calcification analysis showed no significant difference in proportion of area of cartilage matrix and trabecular bone in keel tissue among the 3 groups, but the degree of keel calcification in LP3 was higher than in the other 2 groups. Serum metabolomics showed 32 and 28 differentially accumulated metabolites (**DAMs**) in the 2 comparison groups, LP1 vs. LP3 and LP1 vs. LP2, respectively. Carboxylic acids and derivatives were the most abundant among the DAMs. Sternal transcriptome analysis showed 231 differentially expressed genes (**DEGs**), including 177 upregulated genes and 54 downregulated genes in group LP1 vs. LP3, and 22 DEGs in group LP1 vs. LP2. Protein-protein interaction (**PPI**) network analysis on DEGs between LP1 and LP3 showed that genes *BTRC, GLI1, BMP4*, and *FOS* were in the core position of the interaction network, and are also involved in bone development. KEGG pathway analysis of DAMs and DEGs showed that differences in Hedgehog signaling pathway, MAPK signaling pathway, apoptosis, energy metabolism, and amino acid metabolism following light treatment seem likely to have contributed to the observed difference in calcification of duck sternum.

Key words: duck, sternal calcification, light supplement, metabolome, transcriptome

2022 Poultry Science 101:101697
https://doi.org/10.1016/j.psj.2022.101697

INTRODUCTION

Domestic animals are prone to bone problems during the rapid growth stage, including fractures, deformities, infections, and osteoporosis, many of which are caused by insufficient bone calcification (Rath et al., 2000; Sitara et al., 2006). Most bones, such as the long bones, are formed by endochondral ossification, in which cartilage during growth is first formed as a template and then replaced by bone (Mackie et al., 2008). Many factors affect the calcification of animal bones, including genetic, nutritional, environmental, and other factors (James et al., 2010; Zhang et al., 2018).

Light is an important environmental parameter in domestic animal production, including light color, light intensity, and light cycle (Olanrewaju et al., 2006). Poultry is sensitive to light information and can receive light information through retinal and non-retinal light receptors (Wilson, 2011). Light plays an important role in the growth, skeletal development, welfare, and reproductive performance of poultry (Deep et al., 2010; Schwean et al., 2012; Vermette et al., 2016; Rault et al., 2017). White and blue light stimulation during incubation had no negative effects on hatchability, embryo mortality, spread of hatch, or day-old chick quality, but

Received May 12, 2021.
Accepted January 5, 2022.

[1]These authors contributed equally as the first author.

[2]Corresponding author: ll457@163.com

may have potential impacts on immunity and energy metabolism in broiler embryos (Li et al., 2021). The layer photo stimulated with 1 lx of light had reduced ovary development and was heavier than their counterparts exposed to 50 and 500 lx (Renema et al., 2001). Broilers in the 200 lx environment were more active and had greater feed intake than those in 1 lx (Blatchford et al., 2012).

Artificial light is one of the critical environmental factors affecting bone calcification in poultry. In a specific range of light intensity, the activity of broilers was positively correlated with light intensity, which increases the pressure and load on bones and promotes bone development (Mohammed et al., 2016; Škrbić et al., 2019). The light can cause changes in some skeletal metabolic pathways, such as calcium and phosphorus metabolism (Tabeekh et al., 2016). Appropriate photoperiods increased body weight, average daily gain, cortical bone generation, and bone mineralization (Cui et al., 2019). The length and weight of the tibiotarsus of broilers were positively affected by intermittent lighting (Yildiz et al., 2009). Circadian incubation lighting schedule can improve leg health in broilers (van der Pol et al., 2017). Increasing light time slowly during the rearing period is more beneficial to the bones of the laying hens than increasing the light time quickly system development (Hester et al., 2011).

Sternum is the largest bone in the poultry skeletal system, which provides the attachment site for pectoral muscle and protects internal organs, such as the heart and lungs (Pourlis and Antonopoulos, 2019). The ducks (Cherry Valley) grow rapidly from 14 to 42 d of age, and the growth slows gradually after 42 d of age. However, the sternum calcifies quickly from 42 to 49 d of age, and it reaches a plateau after 49 d of age (Zhang et al., 2017). Our previous research demonstrated that ducks (Nonghua duck) sterna ossified during 5 to 9 wk old (Wang et al., 2021). Genetic selection for the rapid growth of poultry can improve the weight and meat yield. However, the accelerated growth also brings some problems, such as imbalance of sternum and breast development (Bozkurt et al., 2017). The sternum ossification of ducks at slaughter age is incomplete, accounting for about 80% of the whole process (Zhang et al., 2019b). The slow rate of sternal calcification may lead to respiratory problems and sternal fractures during feeding, slaughtering, and transportation, then cause the health and welfare of ducks (Wideman, 2001; Rufener et al., 2019). In China, consumers prefer duck with a fully calcified sternum. The consistency of sternal calcification in meat ducks is usually insufficient when ducks reach the slaughter weight (Zhang et al., 2019a). Light may be one reason for the difference in sternal calcification among individuals because the light distribution in pens is usually uneven in production (Raccoursier et al., 2019).

This study was to explore the differences in sternal calcification in ducks under different light programs, and was to illustrate the mechanism underlying the calcification process impacted by light regimes by integrating metabolomics and transcriptome methods.

MATERIALS AND METHODS

Ethics Statement

The experimental procedures and protocols that are applied in this study were approved by the Institutional Animal Care and Use Committee (**IACUC**) of Sichuan Agricultural University (Permit No. DKY-B20201302), and carried out in accordance with the approved guidelines.

Experimental Design and Sampling

A total of 162 Cherry Valley ducks (81 males and 81 females) were provided by Sichuan New Mianying Agriculture and Animal Husbandry Co. Ltd (Mianyang, China). Ducks at 14 d of age were divided into 3 groups randomly. Each group had 3 replicates, resulting in 18 individuals per replicate (half males and half females). All ducks were reared in cages (2.0 × 1.3 × 0.7 m) in a temperature- and humidity-controlled breeding house, and had free access to drinking water and feed at 14 to 43 d of age, and feed was restricted at 44 to 51 d of age, with a daily limit of 120 g. Each group was exposed to white LED light for 24 h (24L: 0D) a day. The white LED light has the same power, and the required light intensity is generated by controlling the number of LED lights and the distance between the light and the cage. The light intensity is measured in 11:00 and 20:00 every day, and the light intensity is the average value of the daily measurement. The group LP1 was set as a control group, in which ducks were exposed to 2 lx light intensity from 14 to 51 d of age; the group LP2 provided light intensity of 70 lx from 14 to 29 d of age, 2 lx from 30 to 51 d of age, respectively; the group LP3 provided light intensity of 70 lx from 14 to 43 d of age, 2 lx from 44 to 51 d of age, respectively (Supplementary Figure S1A).

At the age of 52 d, 3 healthy male ducks were selected from each group (1 per replicate) for sampling. After 12 h of fasting, 3 mL of blood was collected from the vein under the wing. Serum was obtained from blood centrifuged at 4°C for 15 min at 3,500 × g, then stored in an ultra-low temperature refrigerator at −80°C for the subsequent metabolomics analysis. Then, all the sampling ducks were weighed and slaughtered. The keel tissues were collected at the lower end of the sternum for calcification analysis. RNA samples were collected at the midpoint of the sternum caudal, keeping the same position for different individual sampling (Supplementary Figure S1B).

Observation of Sternal Calcification

Keel tissues were fixed in 4% paraformaldehyde for more than 24 h, then decalcified in 10% EDTA at room temperature for 9 wk and embedded into paraffin. Serial sections (3 μm) were cut for the subsequent treatment.

Hematoxylin-eosin (**H&E**) staining was performed to visualize the changes in the tissues, the nucleus was stained in blue, and the cytoplasm was in red (Rigueur and Lyons, 2014). The sections were taking panoramic photos with 20 × magnification using Digital Pathology Total Section Scanner (VS120-S6-W, Olympus, Japan), and then calculating the area of different bone tissues (Zhao et al., 2018).

Metabolome Analysis of Serum

Serum samples were thawed at 4°C and 100 μL of each sample was transferred into a 2 mL centrifuge tube, and 400 μL of methanol was added to each tube, then eddied for 60 s. The liquid was centrifuged at 12,000 g for 10 min, transferred 450 μL into another 2 mL centrifuge tube, and concentrated to dryness in a vacuum. Samples were dissolved with 150 μL 2-chlorobenzalanine (4 ppm) methanol solution, and the supernatant was filtered through 0.22 μm membrane to obtain the prepared samples for liquid chromatograph-mass spectrometer (**LC-MS**) (Dunn et al., 2011).

Chromatographic separation was accomplished in a thermal vanquish system equipped with an ACQUITY UPLC HSS T3 (150 × 2.1 mm, 1.8 μm, Waters) column maintained at 40°C. The temperature of the autosampler was 8°C. Gradient elution of analytes was carried out with 0.1% formic acid in water, 0.1% formic acid in acetonitrile (B1), and acetonitrile (B2) at a flow rate of 0.25 mL/min. Injection of 2 μL of each sample was done after equilibration. An increasing linear gradient of solvent B1/B2 (v/v) was used as follows: 0 to 1 min, 2% B1/B2; 1 to 9 min, 2% to 50% B1/B2; 9 to 12 min, 50% to 98% B1/B2; 12 to 13.5 min, 98% B1/B2; 13.5 to 14 min, 98% to 2% B1/B2; 14 to 20 min, 2% B1-positive model (14−17 min, 2% B2-negative model).

The ESI-MSn experiments were executed on the Thermo Q Exactive mass spectrometer with the spray voltage of 3.5 kV and −2.5 kV in positive and negative modes, respectively. Sheath gas and auxiliary gas were set at 30 and 10 arbitrary units, respectively. The capillary temperature was 325°C. The analyzer scanned over a mass range of m/z 81 to 1,000 for a full scan at a mass resolution of 70,000. Data-dependent acquisition (**DDA**) MS/MS experiments were performed with an HCD scan. The normalized collision energy was 30 eV. Dynamic exclusion was implemented to remove some unnecessary information in MS/MS spectra (Zelena et al., 2009).

The raw data were converted into mzXML format by Proteowizard software (v3.0.8789) and used the XCMS package of R (v3.3.2) for peak identification, peak filtration, and peak alignment. The peak area data were normalized within the sample. Pareto conversion processing was performed on metabolomics data to obtain standardized data. The fragment information obtained from MS/MS mode was matched and annotated in human metabolomic database (**HMDB**) (http://www.hmdb.ca), Metlin (http://metlin.scripps.edu), massbank (http://www.massbank.jp/), LipidMaps (http://www.lipidmaps.org), and mzclound (https://www.mzcloud.org) to obtain accurate metabolite information.

The DAMs were screened under the conditions of P-value ≤ 0.05 and Variable importance in the projection (**VIP**) ≥ 1 (Trygg and Wold, 2002). A hierarchical clustering map of relative quantitative values of metabolites was obtained using the pheatmap package in R (v3.3.2). In addition, MetaboAnalyst 5.0 (http://www.metaboanalyst.ca) was used to analyze the metabolic pathways of DAMs.

Transcriptome Analysis of Sternum

According to the manufacturer's instructions, total RNA was isolated using TRIzol reagent (Invitrogen, Carlsbad, CA). Poly (A) + mRNA was purified with mRNA capture beads, and then the mRNA was randomly segmented into small fragments by divalent cations in a fragmentation buffer. These short fragments were used as templates to synthesize the first-strand cDNA using random hexamer primers. Second-strand cDNA was synthesized using RNaseH and DNA polymerase I. Short cDNA fragments were purified with VAHTSTM DNA Clean Beads. The cDNA fragments were then connected with sequencing adapters according to an Illumina protocol (San Diego, CA). After agarose gel electrophoresis, the target fragments of 300 to 500 bp were selected for PCR amplification to create the final cDNA library.

The RNA libraries were prepared using the VAHTS mRNA-seq V3 Library Prep Kit for Illumina according to the product instructions (Jingjing et al., 2014, 2015). First, the quality and size of the cDNA libraries for sequencing were checked using the Agilent 2200 TapeStation system (Beijing, China). Then, cDNA libraries were sequenced on the Illumina sequencing platform (NovaSeq 6000 Illumina). FastQC analyzed raw reads for quality, and high-quality reads with Q >20 were obtained using NGSToolkits (version: 2.3.3; Fumagalli et al., 2014). Finally, functions of the unigenes were annotated based on sequence similarities to sequences in the public UniProt database (Grabherr et al., 2011).

Differentially expressed genes between the 3 groups were identified using the DESeq2 R package. P-value < 0.05 and $\log_2$(fold change) >1 or $\log_2$(fold change) < −1 was set as the threshold for significantly differential expression.

Combined Analysis of Transcriptome and Metabolome

Taking 9 samples as abscissa and the normalized content of DEGs or DAMs as ordinate, each gene and metabolite can construct a curve. The software Short Time-series Expression Miner (version 1.3.13) was used

to conduct cluster analysis on the curves, with a significant level of $P < 0.01$ and the correlation coefficient >0.8. KEGG pathway analysis was carried out for the DEGs and DAMs in the expression profiles that were significantly clustered.

Statistical Analysis

Data were analyzed using the SPSS statistical software version 20.0 (IBM Corp., Armonk, NY). *t* Test and one-way ANOVA were used to analyze the differences between the groups. The data were presented as Mean ± SEM, and $P < 0.05$ was used as a significant statistical difference. SIMCA-P software (version 14.1, Umetrics, Umea, Sweden) was used for Partial Least Squares-Discriminant Analysis (**PLS-DA**) of transcriptome and metabolome data (Etienne et al., 2015).

RESULTS

Calcification of Keel Under Different Light Programs

The histomorphology of the keel near the sternum body is shown in Figure 1. In the control group (LP1), marrow

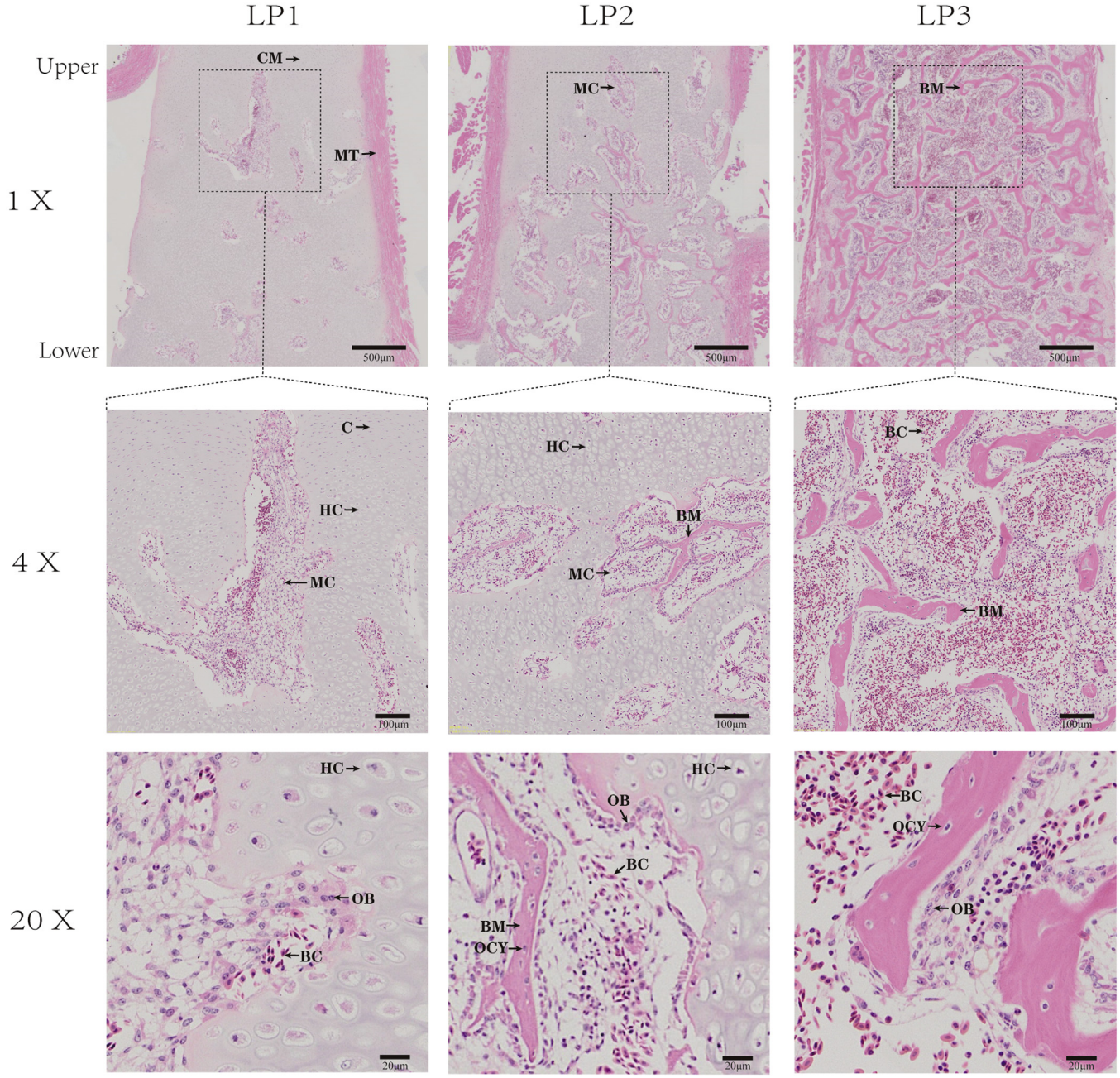

Figure 1. The histology observation of microstructure in keel tissues of ducks under different light supplement modes. Hematoxylin-eosin staining (magnification, 1 ×, 4 ×, 20 ×). Abbreviations: BC, blood cells; BM, bone matrix (trabecular bone); C, chondrocyte; CM, cartilage matrix; HC, hypertrophic chondrocytes; MT, muscle tissue; MC, marrow cavities; OCY, osteocytes; OB, osteoblasts.

Table 1. Effects of light programs on histomorphology parameters of sternum tissue.

Variable	LP1	LP2	LP3	*P*-value
CM.Ar,%	79.73 ± 15.3	62.26 ± 16.5	36.43 ± 17.9	0.125
HC.Ar,%	16.53 ± 12.1	16.10 ± 6.4	16.74 ± 5.1	0.96
MC.Ar,%	3.68 ± 3.1	18.59 ± 10.4	36.7 ± 17.8	0.11
TB.Ar,%	0.05 ± 0.05	3.04 ± 2.4	10.11 ± 5.3	0.086

Abbreviations: CM.Ar, percent cartilage matrix area; HC.Ar, percent hypertrophic chondrocytes area; MC.Ar, percent marrow cavity area; TB.Ar, percent trabecular bone area.

Data are represented as Mean ± SEM (n = 3).

cavities appeared, surrounded by hypertrophic chondrocytes, there were many osteoblasts and blood cells in the marrow cavities. The area of marrow cavities in LP2 was more than those in LP1, bone trabecula appeared in marrow cavity and osteocytes were embedded in it. In LP3 group, there were more trabecular bones and osteocytes, and the hypertrophic chondrocytes have apoptosis. The static parameters of bone histomorphology were analyzed (Table 1). Panoramic detection images of keel sections can be divided into cartilage matrix area, hypertrophic chondrocytes area, marrow cavities area, and trabecular bone area. The proportion of the area of each part was separately counted, and the results showed no significant difference in these bone compositions between the 3 groups. Still, the LP3 had the lowest percent cartilage matrix area and the highest percentage of marrow cavities area and trabecular bone area (Table 1).

Overview of Metabolome and Transcriptome Dataset

The base peak chromatogram of serum metabolites of a typical sample shows the difference in the appearance time and peak area of each peak between the 3 groups (Supplementary Figure S2), indicating that the type and concentration of metabolites in different groups were quite different. A total of 9 cDNA libraries were synthesized, and transcriptome RNA-sequencing (**RNA-seq**) data were generated. The RNA-seq yielded a total of 56.97 Gb clean reads with 96.69% of bases scoring Q30 and above (Supplementary Table S1). In addition, 54.32% of the total clean reads were mapped in proper pairs with the duck reference genome (*Anas platyrhynchos*) (Supplementary Table S2).

PLS-DA indicated that PC1 of the metabolites accounted for 19.9% of the variation (Figure 2A) and that PC1 of the transcripts accounted for 41.5% of the variation (Figure 2C). The samples were clustered well within the group, which indicated that the repeatability is well and the quality of the sample is reliable. The R2 and Q2 values of PLS-DA model were greater than 0.5 and 0.4, respectively (Supplementary Table S3), which suggested that the PLS-DA model was established successfully (Anne-Laure and Korbinian, 2007). Permutation test plot can help evaluate whether the current PLS-DA model is overfitting effectively. The evaluation criteria are (satisfy any one of them): 1) All the blue Q2 points were lower than the rightmost original blue Q2 point; 2) The regression line of Q2 point is less than or equal to zero at the intersection of ordinates. Our results meet the requirements above (Figures 2B and2D), suggesting that the model was not overfitting.

Analysis of DAMs Between Different Light Programs

LC-MS detected 2,070 kinds of metabolites in the serum of the 3 groups. According to molecular weight and matching annotations in the database, 335 metabolites were annotated. The metabolites can be classified into 14 classes, including Carboxylic acids and derivatives, Fatty Acyls, Organooxygen compounds, and Phenols, etc. (Supplementary Figure S3).

Screening of DAMs between the 3 groups, there were 32 and 28 DAMs in group LP1 vs. LP3 and group LP1 vs. LP2, respectively (Figure 3A). We classified the DAMs and found that carboxylic acids and derivatives had the largest number (Figures 3B and 3C). The regions with different colors in the heatmap represent distinct clustering and grouping information (Figure 3D). The metabolic patterns within the same group are similar, which may have similar functions or participate in the same biological processes.

To further investigate the biological processes of the DAMs participated in, KEGG pathway enrichment analysis was conducted in this study. DAMs in group LP1 vs. LP3 were enriched in the Alanine, aspartate and glutamate metabolism (gga00250), Beta-Alanine metabolism (gga00410), Arginine biosynthesis (gga00220), D-Glutamine and D-glutamate metabolism (gga00471), TCA cycle (gga00020), and Histidine metabolism (gga00340) (Figure 4A). The results showed that supplementary light during 14 to 43 days old mainly affects the amino acid metabolism and energy metabolism of duck. For group LP1 vs. LP2, DAMs were notably enriched in the Gap junction (gga04540), Ferroptosis (gga04216), Alanine, aspartate and glutamate metabolism (gga00250), FoxO signaling pathway (gga04068), Regulation of actin cytoskeleton (gga04810), and Arginine and proline metabolism (gga00330) (Figure 4B).

Analysis of DEGs Between Different Light Programs

The DESeq2 packages were used to identify the DEGs in comparison groups LP1 vs. LP3 and LP1 vs. LP2. After comparison, we obtained 231 DEGs between LP1 and LP3, including 177 upregulated and 54 downregulated genes (Figure 5A). A total of 22 DEGs were obtained between LP1 and LP2, including 12 upregulated and ten downregulated genes (Figure 5C).

Functional classification of DEGs was achieved using a gene ontology (**GO**) analysis via DAVID v6.8 (Huang et al., 2009). DEGs in group LP1 vs. LP3 were mainly related to development, including transcriptional

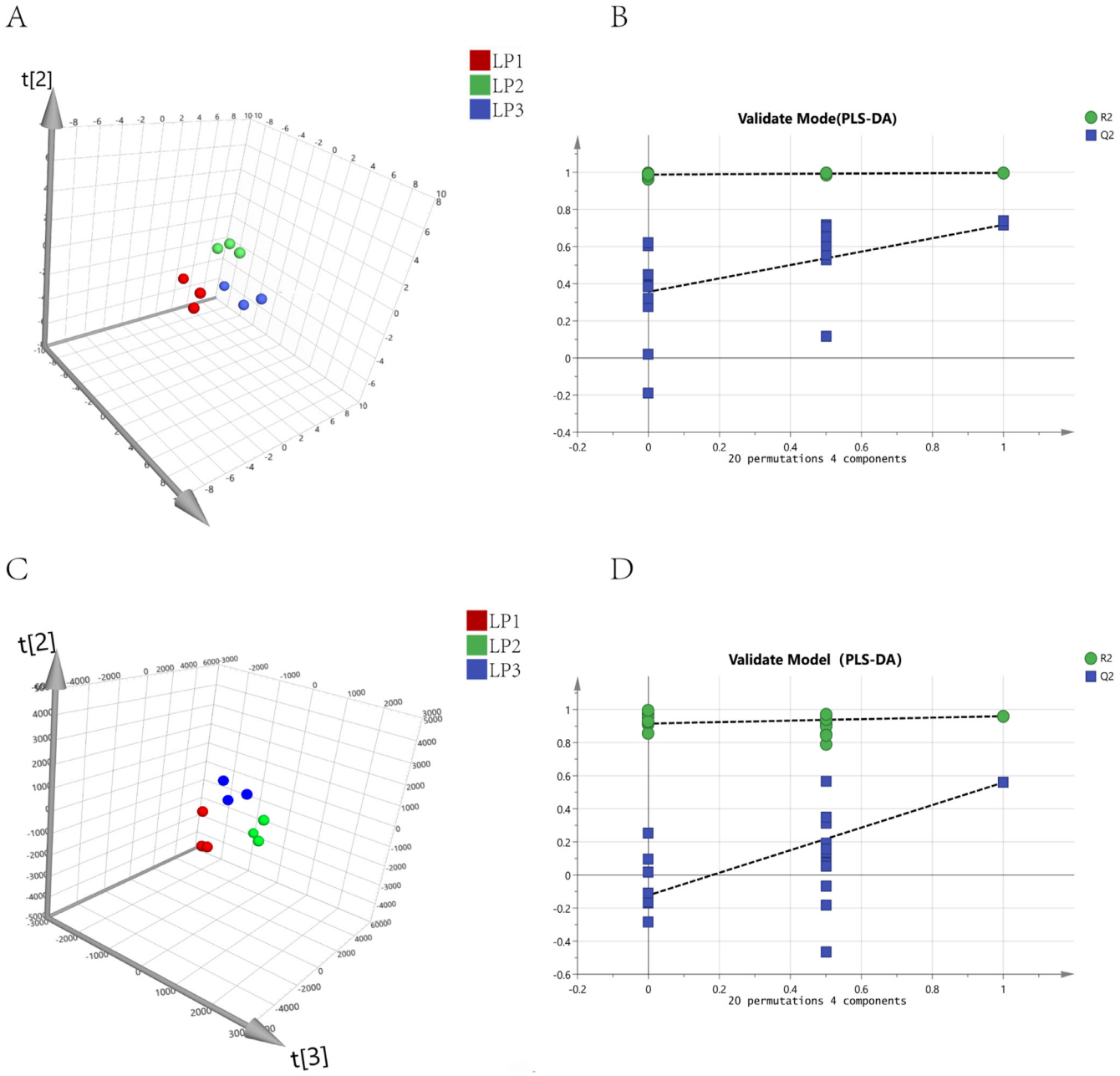

Figure 2. Multivariated statistical analysis based on Count-Per-Millon (CPM) data. (A) PLS-DA score plot of LP1, LP2, and LP3 group in metabolomics (positive ion mode) analysis. (B) Permutation test plot of LP1, LP2, and LP3 group in metabolomics analysis. The x-axis represents the correlation coefficient between the original y-variable and the permuted y-variable, the y-axis represents the cumulative R2 and Q2 of the correlation coefficient. (C) PLS-DA score plot of LP1, LP2, and LP3 group in transcriptome analysis. (D) Permutation test plot of LP1, LP2, and LP3 group in transcriptome analysis. The x-axis represents the correlation coefficient between the original y-variable and the permuted y-variable, the y-axis represents the cumulative R2 and Q2 of the correlation coefficient.

regulation (GO:0045893), nervous system development (GO:0001843, GO:0010001), bone development (GO:0060348, GO:0048701), and other functions (Figure 5B). Pathway enrichment of DEGs was achieved using KEGG enrichment via KOBAS 3.0.11 with the condition of P-value < 0.05 (Xie et al., 2011). Most pathways were associated with bone development, apoptosis, and energy metabolism, such as Hedgehog signaling pathway (apla04340), MAPK signaling pathway (apla04010), Calcium signaling pathway (apla04020), Apoptosis (apla04210), and Pyruvate metabolism (apla00620) (Figure 5D). GO and KEGG analysis in group LP1 vs. LP2 was showed in Supplementary Figure S4.

To study the regulatory network of 231 DEGs of LP1 vs. LP3 and screen the core genes, we performed PPI network analysis on DEGs using the String database (Version 11.0) with a filter threshold of 0.4. We found that genes *BTRC, GLI1, BMP4*, and *FOS* were in the core position of the interaction network (Supplementary Figure S5). Interestingly, these genes were all involved in the pathways related to bone

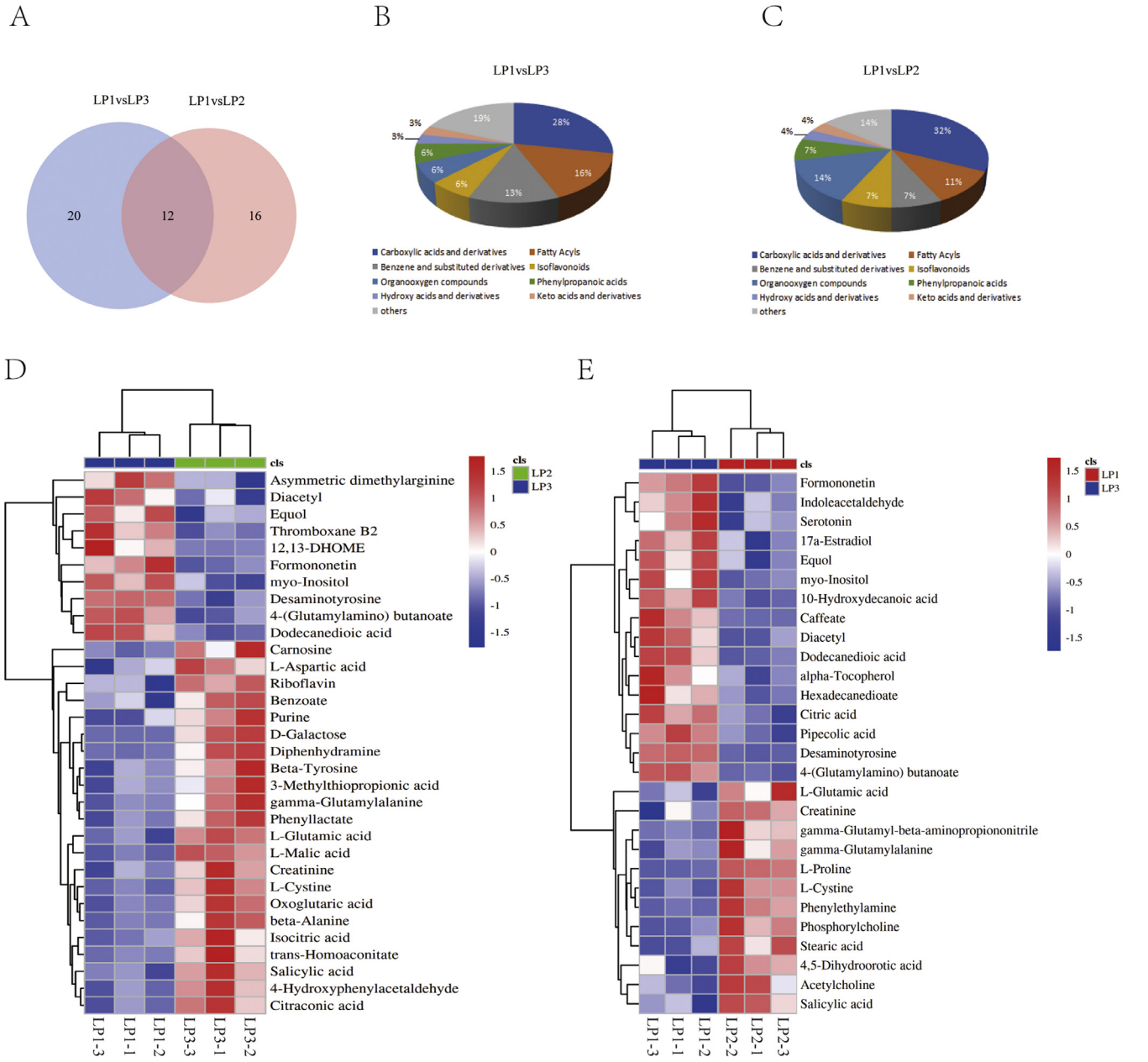

Figure 3. Classification of the DAMs. (A) Venn graph for DAMs in group LP1 vs. LP3 and group LP1 vs. LP2. (B) Pie graph for classification of DAMs in group LP1 vs. LP3. (C) Pie graph for classification of DAMs in group LP1 vs. LP2. (D) Heatmap of DAMs for LP1 vs. LP3. (E) Heatmap of DAMs for LP1 vs. LP2. Abbreviation: DAMs, differentially accumulated metabolites.

development, indicating that they play an essential role in the physiological regulation in sternum development under light supplement.

Association Analysis of Metabolome and Transcriptome Data

Cluster analysis of DEGs and DAMs of LP1 vs. LP3 was performed. We constructed curves for the contents of DEGs (231) and DAMs (32) in 9 ducks. A total of 263 curves were obtained. Using Short Time-series Expression Miner (v1.3.13) software to perform cluster analysis on the curves, we obtained 50 profiles, and 3 of them were statistically significant (Supplementary Figure S6). It suggests that gene expression and serum metabolites are closely related. KEGG pathways of DEGs and DAMs of each profile were enriched, respectively. The profile 10 includes 75 genes and 10 metabolites, Hedgehog signaling pathway was enriched from the genes, and TCA cycle was enriched from the metabolites (Figure 6), both pathways were upregulated, indicating that the changes of the 2 pathways were closely related after light supplement. Similarly, the MAPK signaling pathway and Histidine metabolism were closely related in profile 46 (Figure 6).

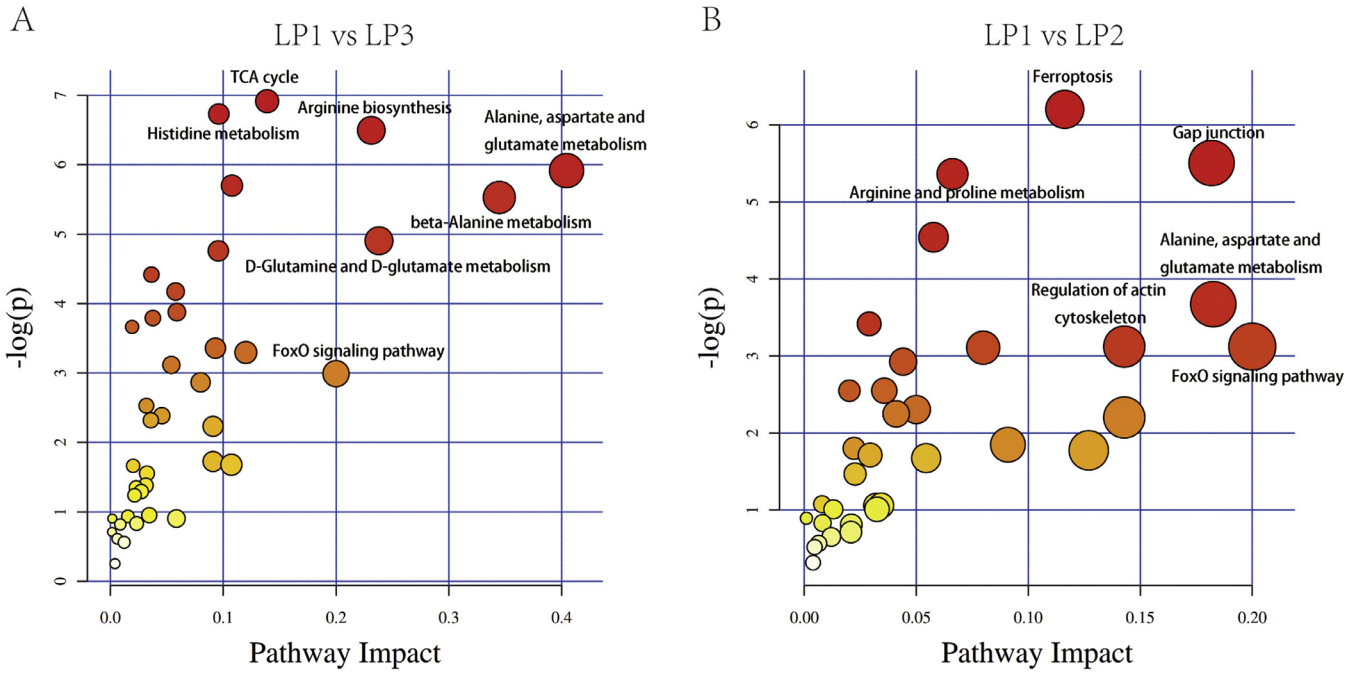

Figure 4. KEGG pathway enrichment analysis of the DAMs in group LP1 vs. LP3 (A) and group LP1 vs. LP2 (B). Abbreviation: DAMs, differentially accumulated metabolites.

DISCUSSION

Birds are sensitive to light and can receive light information through retinal and nonretinal light receptors, thus causing metabolic changes (Wilson, 2011). Light at night is a stressor that influences oxidative stress, which can cause the change of redox state in mice liver (Ashkenazi and Haim, 2013). Compared with a single light, blue-green mixed-light significantly improved the serum glucose level of birds (Yang et al., 2016). In addition, the activities of alkaline phosphatase and tartrate-resistant acid phosphatase, and the contents of transforming growth factor-β (**TGF-β**), osteocalcin, and tumor necrosis factor-α in duck serum increased in ≥12 h photoperiods (Cui et al., 2019). Similarly, in our study, supplemental light induced changes in serum metabolites, mainly including Carboxylic acids and derivatives, Fatty Acyls, and Benzene and substituted derivatives (Figures 3B and 3C). Light has a broad effect on birds, such as growth, sexual maturity, stress, and reproductive performance (Deep et al., 2010; Schwean et al., 2012; Vermette et al., 2016; Rault et al., 2017). In our study, all annotated DAMs belong to various metabolite categories, suggesting that supplementary light affected various metabolic processes of ducks.

In order to compare the differences of sternal calcification among the groups, we used the proportion of area of cartilage matrix, hypertrophic chondrocytes, marrow cavity, and trabecular bone in keel tissue as an index to compare the rate of sternal calcification. The sternal calcification pattern belongs to endochondral bone formation (Shawn et al., 2019), which is a complex physiological process. The process includes chondrocytes stopping proliferating and becoming hypertrophic, perichondria cells adjacent to hypertrophic chondrocytes become osteoblasts, and marrow cavity appears (Yoshifumi and Masaoki, 1999; Ishijima et al., 2012). Hypertrophic chondrocytes attract blood vessels and then undergo apoptosis. The cartilage matrix left behind provides a scaffold for osteoblasts. Osteoblasts differentiate into osteocytes, and calcified bone matrix replaces cartilage matrix (Mackie et al., 2008; Long and Ornitz, 2013).

Light is an essential factor affecting bone development (Cui et al., 2019). In our study, the LP3 group had the highest sternal calcification degree. Similar to our findings, Pullets exposed to the slow lighting photoperiod had longer bones and more bone area than those exposed to the rapid photoperiod (Hester et al., 2011). The light supplement time of LP3 was 14 to 43 d duck age, which was in the particular stage of sternum calcification of duck (Bozkurt et al., 2017). However, during the whole period of the light supplement of LP2, the sternum had not begun to calcify. Therefore, we deduced that light supplements during bone calcification can promote sternal calcification in ducks.

The result of the sternal transcriptome was similar to that of phenotype. The number of DEGs in group LP1 vs. LP2 is far less than that of LP1 vs. LP3. The results showed that light supplement at the early growth stage had little effect on gene expression of the sternum of ducks at 52 days old, which might be related to the fact that the sternum had not started calcification during light supplementation, so we focused on the analysis of LP1 vs. LP3. Some genes related to bone development were found and some significant pathways enriched in transcriptome. In our study, the Hedgehog signaling

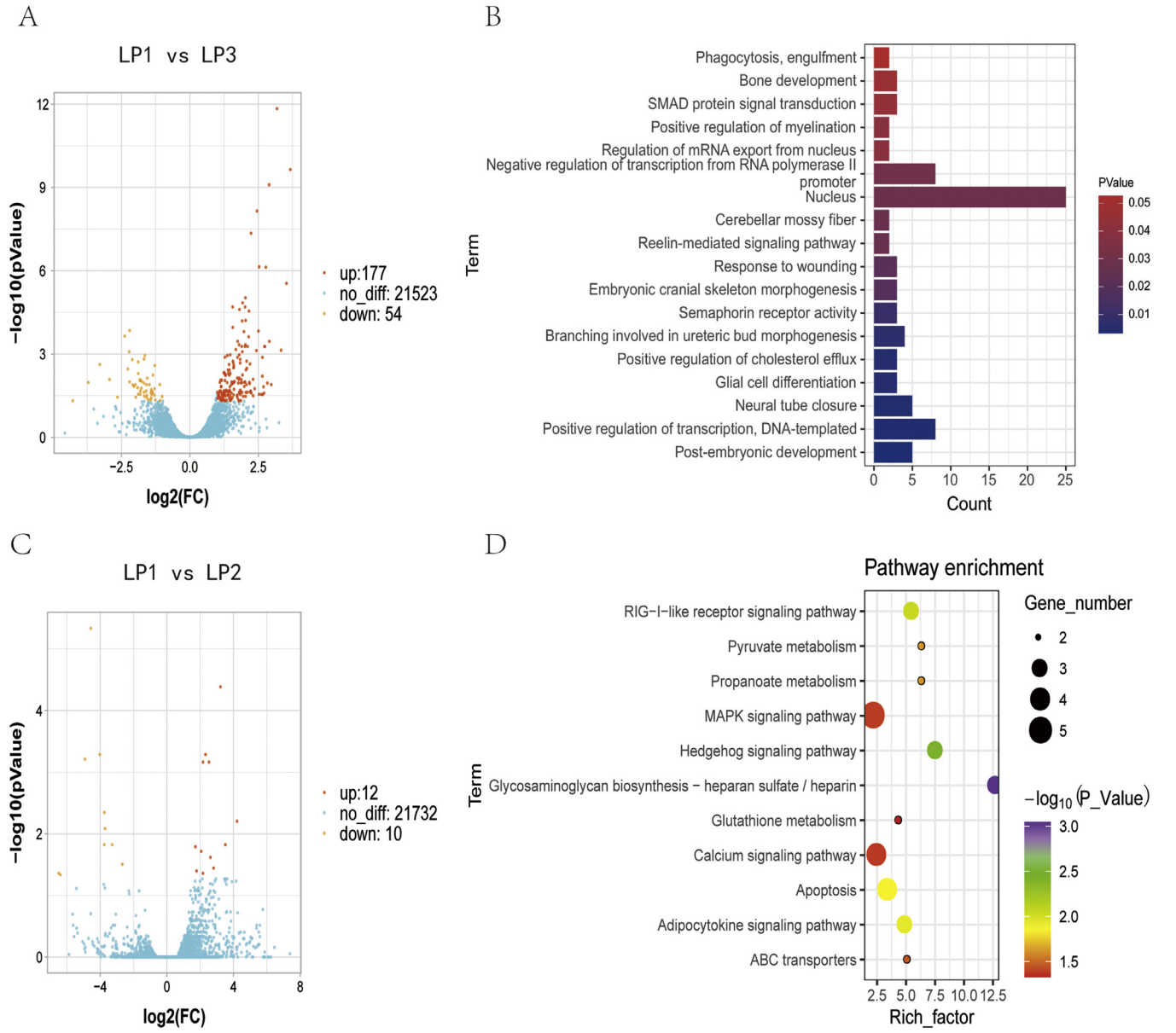

Figure 5. Transcriptome analysis of duck sternum under the condition of supplemental light. (A) Volcano plots of genes in group LP1 vs. LP3. (B) GO analysis of DEGs between LP1 and LP3 (P-value < 0.05). (C) Volcano plots of genes in group LP1 vs. LP2. (D) KEGG pathways bsed on DEGs between LP1 and LP3 (P-value < 0.05). Abbreviations: DEGs, differentially expressed genes; GO, gene ontology

pathway was upregulated. It helps to pattern the limbs and plays a critical part in coordinating chondrocyte proliferation, chondrocyte differentiation, and osteoblast differentiation (Kronenberg, 2003; Alman, 2015). Sonic hedgehog (**Shh**) can induce osteoblast differentiation and ectopic bone formation (Kinto et al., 1997). *BTRC, GLI1*, and *PTCH1* belong to this pathway, and *BTRC* is also in the core position of PPI network of DEGs (Supplementary Figure S5). Thus, we deduce that *BTRC* is a vital gene that mediates light on sternal development.

The mitogen-activated protein kinase (**MAPK**) signaling pathway was also upregulated in LP1 vs. LP3. MAPK can activate runt-related transcription factor (**Runx**)-2 by phosphorylation, which plays a critical role in the differentiation of cells toward an osteoblastic pathway (Canalis et al., 2003; Nishimura et al., 2012; Long and Ornitz, 2013). In our study, *TRADD, ERBB4*, and *FOS* belong to the MAPK signaling pathway. TGF-β signaling pathway was also enriched, members of which are essential in skeletal development, regulating cell proliferation, apoptosis, differentiation, and migration (Chang et al., 2002). In addition, TGF-β can activate Smad-independent pathways, such as those dependent on Ras/MAPK signaling (Wagner and Aspenberg, 2011; Nishimura et al., 2012). In our study, *BMP4* and *SMAD9* belong to the TGF-β signaling pathway.

To study the association between the transcriptome and metabolome in duck, we analyzed the connection of DEGs and DAMs in group LP1 vs. LP3. Similar to the transcriptome analysis results, we observed that the DAMs were also enriched in the Propanoate metabolism, Pyruvate metabolism, ABC transporters,

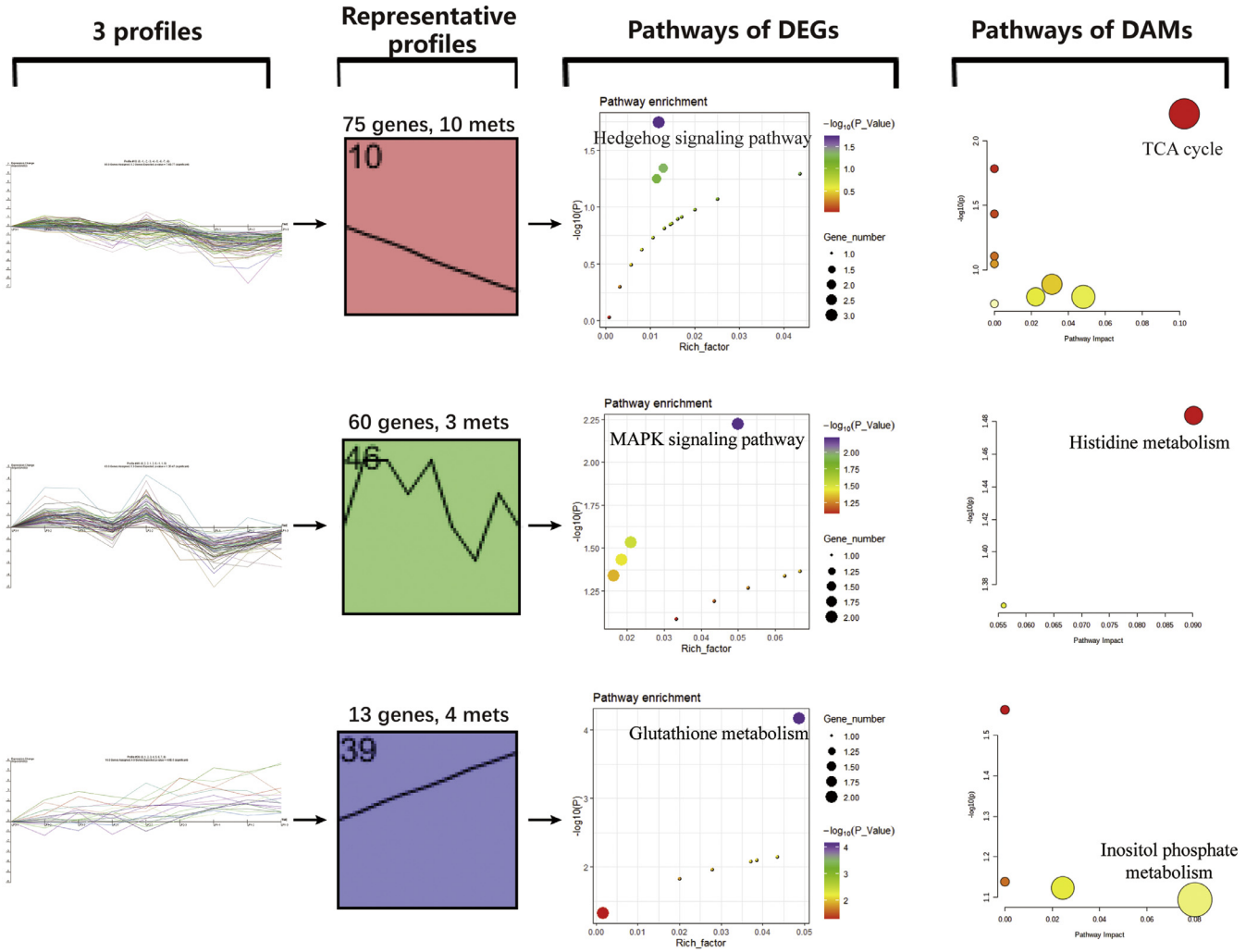

Figure 6. Cluster analysis of DEGs and DAMs of LP1 vs. LP3. Each curve in the profiles represents a gene or metability, the abscissa is the 9 samples, and the ordinate is the normalized value of gene expression or metabolite content. Abbreviations: DEGs, differentially expressed genes; DAMs, differentially accumulated metabolites.

and Glutathione metabolism pathways, mainly related to energy metabolism. The result showed that the changes in metabolite accumulation were tightly governed by differential gene expression. The energy metabolism level of the whole body changed after supplementing light, which may be related to bone development.

CONCLUSIONS

In summary, compared with the environment with low light intensity of 2 lx, supplementing 70 lx LED lighting during duck sternal calcification can improve the calcification rate of duck sternum. Light treatment altered the contents of some metabolites in the serum, including carboxylic acids and derivatives, and also changed the expression of genes such as *BTRC, GLI1, BMP4,* and *FOS*. Integrated analysis of serum metabolome and sternal tissue transcriptome show that supplementing light mainly affected the pathway of Hedgehog signaling, MAPK signaling, Apoptosis, energy metabolism, and amino acid metabolism, ultimately changing the speed of sternal calcification.

ACKNOWLEDGMENTS

This work was supported by the China Agricultural Research System (CARS-42-4), Key Technology Support Program of Sichuan Province (2021YFYZ0014), Key Technologies for Producing High Quality Meat Ducks in Three-dimensional Cage (2020YFN0084)

DISCLOSURES

No conflict of interest exits in the submission of this manuscript, and manuscript is approved by all authors for publication.

SUPPLEMENTARY MATERIALS

Supplementary material associated with this article can be found in the online version at doi:10.1016/j.psj.2022.101697.

REFERENCES

Alman, B. A. 2015. The role of hedgehog signalling in skeletal health and disease. Nat. Rev. Rheumatol 11:552–560.

Anne-Laure, B., and S. Korbinian. 2007. Partial least squares: a versatile tool for the analysis of high-dimensional genomic data. Brief. Bioinform 8:32–44.

Ashkenazi, L., and A. Haim. 2013. Effect of light at night on oxidative stress markers in Golden spiny mice (Acomys russatus) liver. Comp. Biochem. Physiol. A Mol. Integr. Physiol 165:353–357.

Blatchford, R. A., G. S. Archer, and J. A. Mench. 2012. Contrast in light intensity, rather than day length, influences the behavior and health of broiler chickens. Poult. Sci 91:1768–1774.

Bozkurt, M., S. Yalçin, B. Koçer, A. E. Tüzün, H. Akşit, S. Özkan, M. Uygun, G. Ege, G. Güven, and O. Yildiz. 2017. Effects of enhancing vitamin D status by 25-hydroxycholecalciferol supplementation, alone or in combination with calcium and phosphorus, on sternum mineralisation and breast meat quality in broilers. Br. Poult. Sci. 58:452–461.

Canalis, E., A. N. Economides, and E. Gazzerro. 2003. Bone morphogenetic proteins, their antagonists, and the skeleton. Endocr. Rev 24:218–235.

Chang, H., C. W. Brown, and M. M. Matzuk. 2002. Genetic analysis of the mammalian transforming growth factor-β superfamily. Endocr Rev 23:787–823.

Cui, Y.-M., J. Wang, H.-J. Zhang, J. Feng, S.-G. Wu, and G.-H. Qi. 2019. Effect of photoperiod on growth performance and quality characteristics of tibia and femur in layer ducks during the pullet phase. Poult. Sci 98:1190–1201.

Deep, A., K. SchweanLardner, T. G. Crowe, B. I. Fancher, and H. L. Classen. 2010. Effect of light intensity on broiler production, processing characteristics, and welfare. Poult. Sci 89:2326–2333.

Dunn, W. B., D. Broadhurst, P. Begley, E. Zelena, S. Francis-McIntyre, N. Anderson, M. Brown, J. D. Knowles, A. Halsall, J. N. Haselden, A. W. Nicholls, I. D. Wilson, D. B. Kell, and R. Goodacre. 2011. Procedures for large-scale metabolic profiling of serum and plasma using gas chromatography and liquid chromatography coupled to mass spectrometry. Nat. Protoc 6:1060–1083.

Etienne, A. T., R. Aurélie, X. Ying, E. Eric, and J. Christophe. 2015. Analysis of the human adult urinary metabolome variations with age, body mass index, and gender by implementing a comprehensive workflow for univariate and opls statistical analyses. J. Proteome Res 14:3322–3335.

Fumagalli, M., F. G. Vieira, T. Linderoth, and R. Nielsen. 2014. ngsTools: methods for population genetics analyses from next-generation sequencing data. Bioinformatic 30:1486–1487.

Grabherr, M. G., B. J. Haas, M. Yassour, J. Z. Levin, D. A. Thompson, I. Amit, X. Adiconis, L. Fan, R. Raychowdhury, Q. Zeng, Z. Chen, E. Mauceli, N. Hacohen, A. Gnirke, N. Rhind, F. Di Palma, B. W. Birren, C. Nusbaum, K. Lindblad-Toh, N. Friedman, and A. Regev. 2011. Full-length transcriptome assembly from RNA-Seq data without a reference genome. Nat. Biotechnol 29:644–652.

Hester, P. Y., D. A. Wilson, P. Settar, J. A. Arango, and N. P. O'Sullivan. 2011. Effect of lighting programs during the pullet phase on skeletal integrity of egg-laying strains of chickens. Poult. Sci 90:1645–1651.

Huang, D. W., B. T. Sherman, and R. A. Lempicki. 2009. Systematic and integrative analysis of large gene lists using DAVID bioinformatics resources. Nat. Protoc 4:44–57.

Ishijima, M., N. Suzuki, K. Hozumi, T. Matsunobu, K. Kosaki, H. Kaneko, J. R. Hassell, E. Arikawa-Hirasawa, and Y. Yamada. 2012. Perlecan modulates VEGF signaling and is essential for vascularization in endochondral bone formation. Matrix Biol 31:234–245.

James, C. G., L.-A. Stanton, H. Agoston, V. Ulici, T. M. Underhill, and F. Beier. 2010. Genome-wide analyses of gene expression during mouse endochondral ossification. PloS One 5:e8693.

Jingjing, J., P. Deepa, W. Qian, K. M. Jung, L. Jun, Y. Jun-Lin, W. Limsoon, J. In-Cheol, C. Nam-Hai, and S. Rajani. 2014. Next generation sequencing unravels the biosynthetic ability of spearmint (Mentha spicata) peltate glandular trichomes through comparative transcriptomics. BMC Plant Biol 14:292.

Jingjing, J., K. M. Jung, D. Savitha, T. J. Gambino, Y. Jun-Lin, W. Limsoon, S. Rajani, C. Nam-Hai, and J. In-Cheol. 2015. The floral transcriptome of ylang ylang (Cananga odorata var. fruticosa) uncovers biosynthetic pathways for volatile organic compounds and a multifunctional and novel sesquiterpene synthase. J. Exp. Bot 66:3959–3975.

Kinto, N., M. Iwamoto, M. Enomoto-Iwamoto, S. Noji, H. Ohuchi, H. Yoshioka, H. Kataoka, Y. Wada, G. Yuhao, H. E. Takahashi, S. Yoshiki, and A. Yamaguchi. 1997. Fibroblasts expressing Sonic hedgehog induce osteoblast differentiation and ectopic bone formation. FEBS Lett 404:319–323.

Kronenberg, H. M. 2003. Developmental regulation of the growth plate. Nature 423:332–336.

Li, X., B. Rathgeber, N. McLean, and J. MacIsaac. 2021. Providing colored photoperiodic light stimulation during incubation: 1. Effects on embryo development and hatching performance in broiler hatching eggs. Poult. Sci 100:101336.

Long, F., and D. M. Ornitz. 2013. Development of the endochondral skeleton. Cold Spring Harb. Perspect. Biol 5:a008334.

Mackie, E. J., Y. A. Ahmed, L. Tatarczuch, K.-S. Chen, and M. Mirams. 2008. Endochondral ossification: how cartilage is converted into bone in the developing skeleton. Int J Biochem. Cell Biol 40:46–62.

Mohammed, H., M. Ibrahim, and A.-S. Saleem. 2016. Effect of different light intensities on performance, welfare and behavior of turkey poults. J Adv Vet. Anim Res 3:18–23.

Nishimura, R., K. Hata, T. Matsubara, M. Wakabayashi, and T. Yoneda. 2012. Regulation of bone and cartilage development by network between BMP signalling and transcription factors. J. Biochem 151:247–254.

Olanrewaju, H. A., J. P. Thaxton, W. A. Dozier, J. Purswell, W. B. Roush, and S. L. Branton. 2006. A review of lighting programs for broiler production. Int. J. Poult. Sci 5:301–308.

Pourlis, A., and J. Antonopoulos. 2019. The ossification of the vertebral column, thorax and sternum in the quail (Coturnix coturnix japonica). Vet. Res. Forum 10:1–7.

Raccoursier, M., Y. V. Thaxton, K. Christensen, D. J. Aldridge, and C. G. Scanes. 2019. Light intensity preferences of broiler chickens: implications for welfare. Animal 13:2857–2863.

Rath, N. C., G. R. Huff, W. E. Huff, and J. M Balog. 2000. Factors regulating bone maturity and strength in poultry. Poult. Sci 79:1024–1032.

Rault, J.-L., K. Clark, P. J. Groves, and G. M. Cronin. 2017. Light intensity of 5 or 20 lux on broiler behavior, welfare and productivity. Poult. Sci 96:779–787.

Renema, R. A., F. E. Robinson, H. H. Oosterhoff, J. J. R. Feddes, and J. L Wilson. 2001. Effects of photostimulatory light intensity on ovarian morphology and carcass traits at sexual maturity in modern and antique egg-type pullets. Poult. Sci. 80:47–56.

Rigueur, D., and K. M. Lyons. 2014. Whole-mount skeletal staining. Methods Mol. Biol 1130:113–121.

Rufener, C., S. Baur, A. Stratmann, and M. J. Toscano. 2019. Keel bone fractures affect egg laying performance but not egg quality in laying hens housed in a commercial aviary system. Poult. Sci 98:1589–1600.

Schwean, L., K, B. I. Fancher, and H. L. Classen. 2012. Impact of daylength on the productivity of two commercial broiler strains. Br. Poult. Sci 53:7–18.

Shawn, A. H., O. Wanida, and O. Noriaki. 2019. Growth plate chondrocytes: skeletal development, growth and beyond. Int. J. Mol. Sci 20:6009.

Sitara, D., M. S. Razzaque, R. St-Arnaud, W. Huang, T. Taguchi, R. G. Erben, and B. Lanske. 2006. Genetic ablation of vitamin D activation pathway reverses biochemical and skeletal anomalies in Fgf-23-null animals. Am. J. Pathol 169:2161–2170.

Škrbić, Z., M. Lukić, V. Petričević, S. Bogosavljević-Bošković, S. Rakonjac, V. Dosković, and N. Tolimir. 2019. Effects of light

intensity in different stocking densities on tibial measurements and incidence of lesions in broilers. Biotechnol. Anim. Husbandry 35:243–252.

Tabeekh, A., A. Mudhar, and R. J. Abbas. 2016. The effect of color light and stocking density on tibial measurements and levels of calcium and phosphorus in bone and serum of broilers and layers chickens. J. Sci. Technol. 143:1–7.

Trygg, J., and S. Wold. 2002. Orthogonal projections to latent structures (O-PLS). J Chemom 16:119–128.

van der Pol, C. W., I. A. M. van Roovert-Reijrink, G. Aalbers, B. Kemp, and H. van den Brand. 2017. Incubation lighting schedules and their interaction with matched or mismatched post hatch lighting schedules: effects on broiler bone development and leg health at slaughter age. Res. Vet. Sci 114:416–422.

Vermette, C., K. Schwean-Lardner, S. Gomis, T. G. Crowe, and H. L. Classen. 2016. The impact of graded levels of daylength on turkey productivity to eighteen weeks of age. Poult. Sci 95:985–996.

Wagner, D. O., and P. Aspenberg. 2011. Where did bone come from? Acta Orthop 82:393–398.

Wang, Y., K. Wu, X. Gan, Q. Ouyang, Q. Wu, H. Liu, S. Hu, C. Han, R. Zhang, J. Hu, J. Wang, and L. Li. 2021. The pattern of duck sternal ossification and the changes of histological structure and gene expression therein. Poult. Sci 45:101112.

Wideman, R. F. 2001. Pathophysiology of heart/lung disorders: pulmonary hypertension syndrome in broiler chickens. Worlds Poult. Sci. J 57:289–307.

Wilson, M. E. A. 2011. What the bird's brain tells the bird's eye: the function of descending input to the avian retina. Vis. Neurosci 28:337–350.

Xie, C., X. Mao, J. Huang, Y. Ding, J. Wu, S. Dong, L. Kong, G. Gao, C.-Y. Li, and L. Wei. 2011. KOBAS 2.0: a web server for annotation and identification of enriched pathways and diseases. Nucleic Acids Res 39:W316–W322.

Yang, Y., Y. Yu, J. Pan, Y. Ying, and H. Zhou. 2016. A new method to manipulate broiler chicken growth and metabolism: response to mixed LED light system. Sci. Rep 6:25972.

Yildiz, H., M. Petek, G. Sonmez, I. Arican, and B. Yilmaz. 2009. Effects of lighting schedule and ascorbic acid on performance and tibiotarsus bone characteristics in broilers. Turk. J. Vet. Anim. Sci 33:469–476.

Yoshifumi, N., and T. Masaoki. 1999. Development of the skeleton in Japanese quail embryos. Dev. Growth Differ 41:523–534.

Zelena, E., W. B. Dunn, D. Broadhurst, S. Francis-McIntyre, K. M. Carroll, P. Begley, S. O'Hagan, J. D. Knowles, A. Halsall, I. D. Wilson, and D. B. Kell. 2009. Development of a robust and repeatable UPLC-MS method for the long-term metabolomic study of human serum. Anal. Chem 81:1357–1364.

Zhang, H. Y., H. Liao, Q. F. Zeng, J. P. Wang, X. M. Ding, S. P. Bai, and K. Y. Zhang. 2017. A study on the sternum growth and mineralization kinetic of meat duck from 35 to 63 days of age. Poult. Sci 96:4103–4115.

Zhang, H. Y., Q. F. Zeng, S. P. Bai, J. P. Wang, X. M. Ding, Y. Xuan, Z. W. Su, T. J. Applegate, and K. Y. Zhang. 2019b. Calcium affects sternal mass by effects on osteoclast differentiation and function in meat ducks fed low nutrient density diets. Poult. Sci 98:4313–4326.

Zhang, H., H. Liao, Q. Zeng, J. Wang, X. Ding, S. Bai, and K. Zhang. 2019a. Effects of commercial premix vitamin level on sternum growth, calcification and carcass traits in meat duck. J. Anim. Physiol. Anim. Nutr. (Berl) 103:53–63.

Zhang, H., Q. Zeng, S. Bai, J. Wang, X. Ding, Y. Xuan, Z. Su, and K. Zhang. 2018. Effect of graded calcium supplementation in low-nutrient density feed on tibia composition and bone turnover in meat ducks. Br. J. Nutr 120:1217–1229.

Zhao, H., X. Li, D. Zhang, H. Chen, Y. Chao, K. Wu, X. Dong, and J. Su. 2018. Integrative bone metabolomics-lipidomics strategy for pathological mechanism of postmenopausal osteoporosis mouse model. Sci. Rep 8:16456.